



Methane and nitrous oxide emissions from rice grown on organic soils in the temperate zone

Chloé Wüst-Galley^{a,*}, Sandra Heller^{a,b}, Christof Ammann^a, Sonja Paul^a, Sebastian Doetterl^b, Jens Leifeld^a

^a Climate and Agriculture Group, Agroscope, Reckenholzstrasse 191, 8046 Zurich, Switzerland

^b Department of Environmental Systems Science, ETH Zurich, Universitätstrasse 16, 8092 Zurich, Switzerland

ARTICLE INFO

Keywords:

Organic soils
Greenhouse gas mitigation
Chamber flux measurements
Rice cultivation
Agriculture

ABSTRACT

Organic soils are important carbon stocks. The conventional (dry) cultivation of these soils turns them into strong sources of greenhouse gas (GHG) emissions. For situations where restoration of natural land cover is not possible, solutions to this problem include the wet cultivation of these soils, reducing CO₂ and N₂O emissions. One option, paddy rice cultivation, has begun in the Swiss Central Plateau, which hitherto did not provide a suitable climate for wet rice. Wet rice is however associated with high CH₄ emissions. These need to be quantified for this region, as the increased CH₄ fluxes might negate the expected reductions in CO₂ and N₂O. Here, we quantify CH₄ and N₂O emissions from wet rice on organic soil with chamber measurements, in an outdoor mesocosm experiment in the Swiss Central Plateau, located in the cool temperate moist zone. We apply two water treatments (a high water table (WT) treatment, – 6 cm with mid-season drainage, and two medium WT treatments, – 11 and – 17 cm without mid-season drainage) and additionally test the use of a mineral cover layer to reduce N₂O emissions. Additionally, a deeply-drained grassland treatment is used as a reference treatment. Annual CH₄ emissions from rice cultivation are 6.2 g CH₄.m⁻².a⁻¹ for the higher WT treatment, 6.4 g CH₄.m⁻².a⁻¹ for the medium WT treatment and 2.4 g CH₄.m⁻².a⁻¹ for the medium WT treatment with mineral cover. The corresponding N₂O emissions are 203, 190 and 56 mg N₂O-N.m⁻².a⁻¹, respectively. These results show that adding a mineral cover layer reduces annual emissions from both GHGs substantially. In total, the maximum increase in CH₄ and N₂O emissions resulting from rice cultivation, compared to the drained grassland treatment, is 2.3 t CO₂-eq.ha⁻¹.a⁻¹. Expected CO₂ emissions savings (derived from a literature-based model) due to a higher WT are a factor of 5–9 greater than this. We thus conclude that the cultivation of these organic soils in this region with wet rice could reduce their induced warming compared to their cultivation with (deeply drained) grassland.

1. Introduction

Globally, peatlands have in the past had a net cooling effect on the climate (Frolking et al., 2011). Peatland degradation, often through drainage allowing agricultural production, has turned these large carbon (C) pools into strong net greenhouse gas (GHG) sources (Frolking et al., 2011), an effect predicted to increase in the future in the absence of peatland protection strategies (Leifeld et al., 2019; Humpenöder et al., 2020). From several perspectives however, this management is unsustainable (Wijedasa et al., 2016). First, aerobic decomposition of these large C pools results in high CO₂ and N₂O emissions. Indeed, the cultivation of degraded peatland worldwide generates 32 % of cropland GHG emissions, although less than 1 % of cropland occurs on these soils

globally (Carlson et al., 2017). Second, from a management perspective, subsidence, compaction and continued oxidative decomposition of peat following drainage leads to problems for cultivation. These include uneven lowering of the soil surface, resulting in local patches of waterlogged or very dry soils, as well as a reduction of the root zone as the distance between the soil surface and WT decreases. As the effectiveness of the drainage system decreases, drains have to be renewed (Verhoeven and Setter, 2010) often at high costs. The aerobic decomposition of the organic matter eventually leads to a decline in productivity. This, together with their high GHG emissions, provides a strong incentive for the adaptation of agricultural management that respects the wetland character of peatlands (Wijedasa et al., 2016; Freeman et al., 2022).

* Corresponding author.

E-mail address: chloe.wuest@agroscope.admin.ch (C. Wüst-Galley).

<https://doi.org/10.1016/j.agee.2023.108641>

Received 1 April 2023; Received in revised form 12 June 2023; Accepted 20 June 2023

Available online 29 June 2023

0167-8809/© 2024 The Authors. Published by Elsevier B.V. This is an open access article under the CC BY license (<http://creativecommons.org/licenses/by/4.0/>).

Management of the soil WT is critical for determining GHG emissions from organic soils. CH₄ emissions increase strongly as the water level increases and approaches the soil surface, but the concurrent reduction in N₂O and especially CO₂ emissions means there is a GHG optimum close to the surface (Tiemeyer et al., 2020; Evans et al., 2021; Zou et al., 2022). It thus follows that complete or even partial rewetting of organic soils may reduce GHG emissions significantly (Evans et al., 2021). However, partial or complete rewetting impedes or even precludes the conventional use of this land. Paludiculture, broadly defined as biomass production on wet peatlands (Wichtmann et al., 2016), represents a potential alternative form of agriculture that should preserve peat and reduce CO₂ and N₂O emissions while allowing farming to continue. An important issue concerning paludiculture however is its potential negative impact on crop yields. Especially in regions where subsistence farming is practiced, farmers cannot change to a less calorific crop. Likewise, in regions where agricultural land is limited and profit margins high, it is difficult to convince farmers to change to a less profitable crop.

One potential crop might be rice that can withstand dry, waterlogged or flooded conditions. Recently, Swiss farmers have begun to cultivate paddy rice in the wide, flat valley bottoms of the Swiss Central Plateau region, north of the Alps (Jacot et al., 2018). The relatively high yields and profitability, alongside the difficulties of otherwise farming on soils in need of renewed drainage systems, means regional interest from farmers in this crop is increasing.

The cultivation of paddy rice is however associated with high CH₄ emissions. Global rice cultivation generates 8 % of total anthropogenic CH₄ emissions (Saunois et al., 2020), which themselves have caused a 0.5 °C surface temperature increase compared to the 1850–1900 average (Ocko et al., 2021). Indeed, the GHG impact of rice production is about 3 times that of wheat or maize (Linquist et al., 2012). However, if rice were to be grown on partially rewetted organic soils, the GHG balance of cultivating these soils might be improved, as the existing soil C stocks would be protected from further rapid degradation. First, reduced CO₂ emissions (otherwise high on drained organic soils) might offset some or even all of the increased CH₄ emissions. Second, if rice were to be cultivated as ‘wet rice’ i.e. with a high WT but not necessarily flooded, CH₄ emissions might not be excessively high (Freeman et al., 2022).

To date however, there are few reported CH₄ emissions from wet rice cultivation in the cool moist temperate zone, to which the study site belongs, and none from this climate zone in Europe (Bickel et al., 2006; Wang et al., 2018). Additionally, there are only few reports (see Hatala et al., 2012; Knox et al., 2015; Kajjira et al., 2018) of GHG fluxes from wet or flooded rice cultivation outside of the sub-/ tropics (sensu Maclean et al., 2002) on organic soils. This is relevant as CH₄ emissions from wet or flooded rice on organic soils are expected to be higher than on other soil types (Wang et al., 2018).

One measure already used in conventional agriculture to counteract the difficulties of farming degraded peatland soils is the addition of a mineral soil layer on top of the organic soil (Paul and Leifeld, 2022). This measure evens out uneven surfaces, increases the root zone and means that management, especially driving heavy machinery, is less constrained by meteorology. Very few studies on the effects of this practice on CH₄ or N₂O emissions have been carried out and its effects on GHG emissions are unclear (Paul and Leifeld, 2022). Leiber-Sauheitl et al. (2014) found no N₂O emission reduction on organic soils mixed with mineral soil on an extensive pasture in northern Germany, whereas Wang et al. (2022) found a reduction in N₂O emissions of up to 90 % on a meadow covered with a mineral layer in eastern Switzerland.

Here, we present the results of a mesocosm experiment located in the cool temperate moist climate zone in Europe. The use of a mesocosm experiment allows for multiple treatments to be compared at a single site, reducing variation due to site-specific conditions. Using chamber measurements, we compare the CH₄ and N₂O emissions over one year from wet rice cultivation on organic soil, with and without a mineral soil

cover layer, and from conventional (drained) grass cultivation on the same organic soil. We hypothesised that the mineral soil layer would reduce N₂O emissions and that the rice plots with a medium WT would have lower CH₄ emissions than those with the higher WT. Finally, we discuss the GHG balances of the rice and grass plots, using modelled net CO₂ emissions to complement the CH₄ and N₂O measurements. Although we expected rice plots to have higher CH₄ emissions than the grass plots, we expected that these emissions should be offset by the reduced (calculated) CO₂ emissions in rice, resulting from the increased WT.

2. Methods

2.1. The experimental site

The mesocosm experiment is located at Zurich Reckenholz (47.42796° N, 8.51769° E, 444 m a.s.l.) in the eastern part of the Switzerland’s Central Plateau. The mean annual temperature of the site is 9.8 °C (1990–2020) and mean annual precipitation is 1022 mm (see Figs. S1 and S2 for monthly values). The mesocosm is situated outdoors and comprises eight rows of six square concrete-lined holes (each hole or ‘plot’: 1.2 m × 1.2 m × 1.4 m deep). The water level of the six plots in each row is controlled by an automated water control system. The system pumps water into an inspection well at the end of each row and this water seeps into the six plots through a pipe running the length of the six plots, embedded in a gravel bed at the bottom of the each plot. The water level is lowered passively through a drain in the inspection well, but water can be pumped out of the well (and thus the six plots) when necessary, e.g. for pre-harvest drainage. The six plots in each row are thus connected hydrologically. A metal grating at the bottom of each plot (above the water pipe) means the soil in each plot is separated from that of neighbouring plots. The gas measurement chamber covers a surface half the size of the plots (see Section 2.6). A rim, on which the fourth edge of the chamber sits, was therefore created by inserting a concrete slab (5 cm thick, 1.2 m long, 30 cm wide) vertically into the middle of each plot to 25 cm deep (Fig. 1). The resulting subplots were managed identically. One subplot was used for gas measurements and the other subplot used for soil and moisture sensors (see Section 2.5).

2.2. Soil

The 48 concrete-lined plots were filled in March 2020 with degraded fen peat (pH: 6.0; organic C content: 27.4 %; C:N ratio: 19.9:1). The plots with a ‘mineral cover’ treatment were filled only to 30 cm below the surface and the remaining volume filled with a mineral subsoil (silty loamy sand with 12 % clay and 46 % silt; pH: 7.6; organic C content = 0.6 %; C:N ratio = 12.6:1) mixed with 10 kg (dry matter, mass per plot) of greenwaste compost (pH: 8.1; organic C content = 20.5 %, C:N ratio: 13.2:1). The same mineral subsoil had been used to cover meadows over organic soil at a farm in the region. Soil C (%) and total N (%) of the individual plots are given in Table S1. All plots were planted with a grass-clover mix, representing typical management of these soils in the region. The grass was dug into the upper soil layer of all plots in winter 2020–2021.

2.3. Cultivation

The rice breed ‘Loto’ was used for the experiment. This breed can be grown as paddy or upland (dry) rice and is used by farmers in the region. Seedlings were grown in commercially-available potting compost. They were kept in a climate chamber for four weeks and moved to a greenhouse for one week, before being planted out into the mesocosm experiment on 26th May 2021. Planting density was 34 per plot, corresponding to 24 plants / m², typical for this region. Seedlings were fertilised weekly using Wuxal® (Syngenta Agro AG), an NPK mineral fertiliser with micronutrients (K, B, Cu, Fe, Mn, Mo, Zn) receiving in

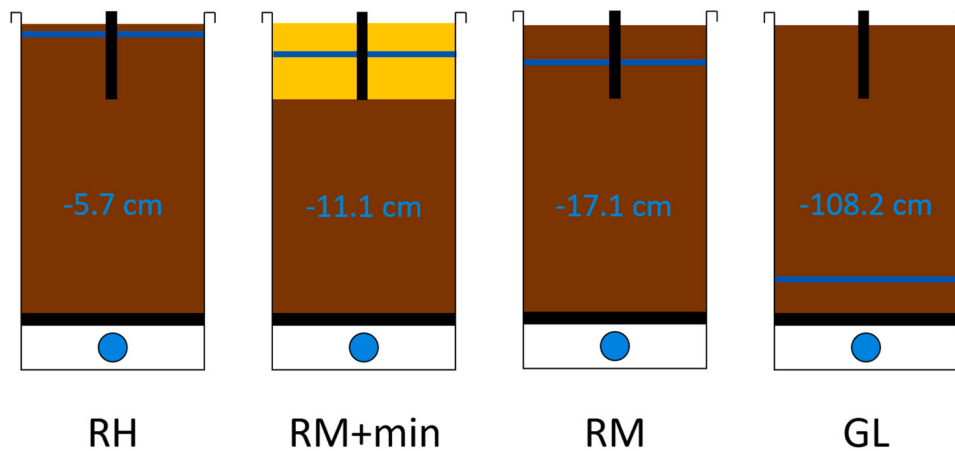


Fig. 1. Schematic diagram showing the cross-sections of plots from the four treatments compared in this study, indicating the calculated water levels (see text for details); RH = rice with high water table (WT), RM+min = rice with medium WT with mineral soil layer, RM = rice with medium WT, GL = grass with low WT; brown = peat, yellow = mineral soil layer, blue line = approx. water level, blue circle = irrigation / drainage pipe, black horizontal line = metal grating, black vertical line = concrete slab inserted to create a rim on which the measurement chamber can sit; note that the water levels refer to levels during period in which these were controlled, and excluding the period of mid-season drainage.

total ca. 26 kg N.ha⁻¹, as nitrate, ammonium, urea and organic N (ratio: 20:29:46:5). Once planted out, the plants received NPK liquid mineral fertiliser (water equivalent to 7 mm precipitation) twice, once on 9th June (5-leaf stage) and once on 13th July (tillering stage), and N fertiliser on 18th August (late booting to heading stage). Total application in the field was – in line with the national fertiliser guidelines (Richner and Sinaj, 2017) – 110 kg N.ha⁻¹, as ammonium nitrate. The plants were harvested (cut ca. 4 cm from plant base) in mid-October 2021, 142–147 days after sowing. Above-ground biomass (including panicles) was dried and weighed.

A commercially-available grass-clover mix (10 % clover, main grass species: *Festuca pratensis*, *Poa pratensis*, *Alopecurus pratensis*, *Lolium perenne* and *Festuca rubra*) was used for the ‘grass’ treatment. This was sown (18th May 2021) two days prior to the first gas measurements. The plots were managed extensively, cut and fertilised twice (fertilised 2–3 days after mowing), receiving a total of 25 kg N.ha⁻¹.

2.4. Water treatment

The water levels for the rice plots were set to be at – 20 cm (treatments with a ‘medium’ WT) and – 5 cm (treatment with a ‘high’ WT) for the vegetation period. The WT for the grass plots was – 110 cm. These automated water levels were initially started on 18th May 2021 but technical problems meant the site had to be drained on 20th May; automation was re-implemented on 28th May. Mid-season drainage was carried out 4th to 12th August (‘high’ WT plots only) and all plots were drained (22nd September) 3–4 weeks prior to harvesting, after which the automated water levels were switched off and plots remained drained.

To calculate WT depths in each plot, water levels (logged in the inspection well of each row) were adjusted to account for soil subsidence of individual plots. Soil subsidence was calculated as the average of monthly measurements (May–September) from the top of the concrete rim to the soil surface. Differential subsidence, as well as a technical limitation of the water control system, meant that the mean calculated water depths for the four treatments deviated from the levels stated above (Fig. 1).

In total, four management options, or treatments, were tested (Fig. 1): Three treatments with rice (4 plots with a high WT [RH], 4 plots with a medium WT [RM], 4 plots with a medium WT with mineral cover [RM+min]) and one treatment with grass (4 grass plots that were deeply drained to – 110 cm [GL]). The 4 plots of each treatment were distributed over 2 rows (i.e. 2 plots per row).

2.5. Soil temperature and moisture

From mid-July onwards, Teros-11® (METER Group) soil sensors buried in each plot at 5 cm depth measured temperature and soil

moisture half-hourly or hourly. The soil temperature before mid-July was derived by calibrating temperature measurements from a nearby (< 30 m) meteorological station (Federal Office of Meteorology and Climatology). The raw outputs from the soil moisture sensors were calibrated to obtain volumetric water content (VWC), using calibration curves for organic and mineral soils separately. These curves were generated according to manufacturer’s instructions, using three soil samples (1 organic, 2 mineral) taken from the experimental site.

The average VWC during the period for which the water levels were controlled were as follows: 0.65 m³.m⁻³ for the RH treatment (excluding the mid-season drainage), 0.63 m³.m⁻³ for the RM treatment and 0.42 m³.m⁻³ for the RM+min treatment (Fig. 2). The reductions in VWC due to the mid-season drainage (VWC at end of drainage vs. average VWC before drainage) were between 15 % and 33 %.

2.6. Gas exchange measurements

CH₄ and N₂O fluxes were measured from May 2021 to May 2022 for rice (for grass, May to October 2021). The first measurements (20th May) took place two days after the grass was sown and six days prior to the planting out of rice seedlings. Measurements were carried out twice weekly (rice) and weekly (grass) during the growing season, and more often around fertilisation events and man-made changes in the WT. For the former, a measurement was carried out one day prior to and one day following fertilisation, and additionally one (for grass) or three (for rice) times in the 10 days following. Monthly measurements were made in the fallow winter season. There was no snow cover at the site on measurement days. In total, for the rice plots, there were 54 measurement days, of which 42 were within the growing season. For the grass plots, there were 26 measurement days. Fluxes from all 12 rice plots or all 4 grass plots were always measured on the same day, between 9 am and 4 pm.

A manual opaque chamber was used for gas sampling, lowered for 15 min per measurement. The chamber (1.2 m × 0.605 m, height 0.795 m, volume 0.5724 m³) sat on the concrete rim of each subplot (see Section 2.1 and Fig. 1). Two fans at the top of the chamber were used to mix the air within the chamber. The air was circulated in a closed loop system to a Picarro G2308 gas analyser (Picarro Inc., USA) which uses cavity ringdown spectroscopy, allowing online gas concentration measurements of CO₂, CH₄ and N₂O (raw precision: CH₄: 10 ppb, N₂O: 25 ppb). N₂ gas was used in the system to ensure dry gas measurements. Our ecosystem respiration measurements were used as quality control for the system (see Section 2.7) and our measurement campaign was not suitable to infer CO₂ emissions.

2.7. Flux calculation

Data checks were carried out as follows. First, the curves of the three

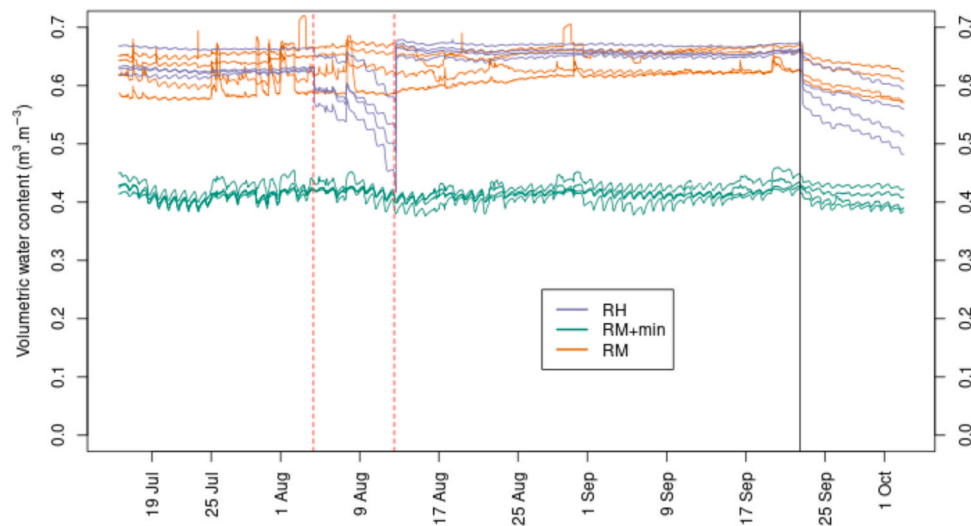


Fig. 2. Volumetric water content of the 12 rice plots from mid-July until the end of September; purple = high water table (WT); green = medium WT with mineral cover; orange = medium WT; red dotted lines = start and end of mid-season drainage (flooded plots only); black vertical line = pre-harvest drainage (all plots).

gases were checked visually. Irregular CH_4 values occurred at the beginning of circa 5 % of measurements. The first 3 min of all measurements (all treatments, all gases) were therefore omitted, resulting in 12 min of data per measurement. Second, the P-values of the slopes of the CO_2 curves were used to check for leaks in the system. Four potentially problematic measurements (or measurement days) were identified. Two of these were single cases (i.e. all other plots were unproblematic on that day) and showed significant CH_4 fluxes. These two cases were retained. On two consecutive measurement days (28th June and 2nd July) several plots showed non-significant CO_2 slopes. A leak in the chamber system was identified and data from these two days discarded. Third, following the flux calculation, fluxes and their confidence intervals (CIs) were used to identify large fluxes with a CI spanning zero, which might be problematic. With one exception, all fluxes with a CI spanning zero (for rice: CH_4 , 3 cases; N_2O , ~ 45 % of measurements) were lower than the MDF of the system and thus deemed unproblematic. The one exception, a CH_4 flux, was only 0.001 $\text{mg CH}_4 \cdot \text{m}^{-2} \cdot \text{h}^{-1}$ greater than the minimal detectable flux (MDF, see below) and was also retained.

The MDF of the system, sensu Maier et al. (2022), was 0.0013 $\text{mg CH}_4 \cdot \text{m}^{-2} \cdot \text{h}^{-1}$ and 0.075 $\text{mg N}_2\text{O} \cdot \text{m}^{-2} \cdot \text{h}^{-1}$. Following Maier et al. (2022), fluxes below the MDF were retained.

The fluxes were calculated using the gasfluxes R package (Hüppi et al., 2018; Fuss, 2020), which automatically selects the most appropriate model to describe the change in gas concentrations, thus avoiding artefacts due to saturation of gases in the headspace. The 'f.detect' parameter was estimated using the simulation method (Fuss, 2020).

Conversion from the change in gas concentration to a gas flux incorporated information on chamber temperature and air pressure. The latter was obtained from the nearby meteorological station (using an average air pressure for the period 9 am–3 pm of each measurement day). The chamber temperature was measured, from the 10th June onwards, using a HOBO temperature logger (Onset Computer Corporation, USA) attached to the chamber. For the (five) measurement days prior to this, calibrated hourly air temperature data from the nearby meteorological station were used.

Annual fluxes were derived from measured fluxes by using linear interpolation to derive continuous fluxes and then by summing these continuous fluxes to generate annual fluxes. In this way, the dominant flux variation – affected most strongly by management activities and season – could be captured. A more complex, driver-based approach was not suitable because no consistent relationships with environmental driver variables were found (data not shown). Annual CH_4 and N_2O

fluxes were converted to CO_2 equivalents using 100-year global warming potentials, CH_4 : 28, N_2O : 273 (Smith et al., 2021). As the GL treatment acted as a 'reference' management option, the mean annual fluxes from that treatment were deducted from those of the rice treatments.

Fertiliser peaks were defined as those N_2O fluxes following a fertilisation event that were higher than the mean flux of the 10 days prior to fertilisation (using upper limit of the confidence interval of the flux), until a flux lower than the mean flux occurred.

2.8. Statistical analysis

The inhomogeneity of variance of the treatments precluded the use of a parametric test. The Kruskal-Wallis test was used to assess whether the three rice treatments had significantly different annual CH_4 and N_2O emissions from one another. Where this was the case ($P < 0.05$), the Games-Howell (post-hoc) test was used to assess the differences between the individual treatments.

3. Results

The hourly flux data (CH_4 and N_2O) are available at Mendeley Data (DOI: 10.17632/fxmnty8zf8.1).

3.1. CH_4 fluxes

After establishment of the wet rice plots, CH_4 fluxes were very low, in the range of -0.05 – 0.14 (mean 0.004) $\text{mg CH}_4 \cdot \text{m}^{-2} \cdot \text{h}^{-1}$ (Fig. 3). Circa one month after the onset of water management and the planting of the seedlings, significant emissions were recorded from all treatments but rose the highest in the RH treatment (mean flux from 1st July to onset of mid-season drainage on 4th August: RH: 5.82 $\text{mg CH}_4 \cdot \text{m}^{-2} \cdot \text{h}^{-1}$; RM+min: 0.64 $\text{mg CH}_4 \cdot \text{m}^{-2} \cdot \text{h}^{-1}$; RM: 0.75 $\text{mg CH}_4 \cdot \text{m}^{-2} \cdot \text{h}^{-1}$). The mid-season drainage of the RH plots decreased CH_4 emissions there, to levels lower than the other two treatments for the same period (mean fluxes 4th to 12th August: RH: 0.37 $\text{mg CH}_4 \cdot \text{m}^{-2} \cdot \text{h}^{-1}$; RM+min: 1.07 $\text{mg CH}_4 \cdot \text{m}^{-2} \cdot \text{h}^{-1}$; RM: 1.37 $\text{mg CH}_4 \cdot \text{m}^{-2} \cdot \text{h}^{-1}$). Following the re-flooding of the RH plots, emissions from that treatment rose to a maximum of only 3.2 $\text{mg CH}_4 \cdot \text{m}^{-2} \cdot \text{h}^{-1}$ (Fig. 3, Fig. S4). In general, the RM and RM+min treatments had lower emissions than the RH treatment (Fig. 3, Figs. S3–5), with the exception of fluxes immediately following the onset of the pre-harvest drainage in September. Here, fluxes of up to 10.1 $\text{mg CH}_4 \cdot \text{m}^{-2} \cdot \text{h}^{-1}$ were measured for the RM+min treatment and up to 97.1 $\text{mg CH}_4 \cdot \text{m}^{-2} \cdot \text{h}^{-1}$ for the RM treatment (Fig. 3, Figs. S3, S5). In the latter treatment, two plots

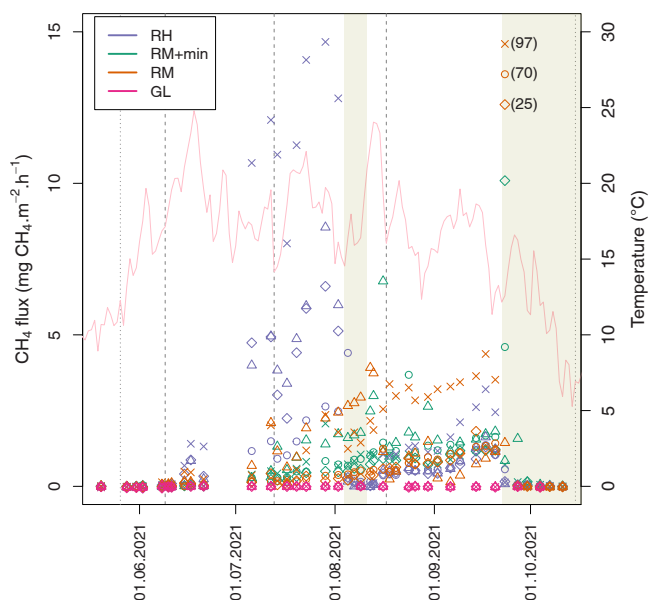


Fig. 3. Hourly CH_4 fluxes ($\text{mg CH}_4\cdot\text{m}^{-2}\cdot\text{h}^{-1}$); RH = plots with a high water table (WT); RM+min = plots with a medium WT with mineral cover; RM = plots with a medium WT; GL = grass plots with a low WT; the four replicates of each treatment are represented by different symbols in the same colour; mean daily temperature shown in pink; fertilisation events shown as vertical dashed lines, planting out of rice plants indicated as vertical dotted line; the beige background shows periods during which either the RH plots were drained (mid-season drainage, early August) or all plots were drained (late September onwards); note that three very high fluxes are shown at the wrong position, with the true flux ($\text{mg CH}_4\cdot\text{m}^{-2}\cdot\text{h}^{-1}$) indicated.

showed extreme values, contributing to 68 % and 84 % of gap-filled emissions of these plots (Fig. 4) and causing the annual CH_4 emissions, on average, to be as high as those of the RH treatment. Across all rice treatments, fluxes fell below $0.16 \text{ mg CH}_4\cdot\text{m}^{-2}\cdot\text{h}^{-1}$ within eight days of the pre-harvest drainage at the end of September. They remained

below $0.06 \text{ mg CH}_4\cdot\text{m}^{-2}\cdot\text{h}^{-1}$ from the beginning of October until the end of the experiment (Fig. 3). Cumulative fluxes during the fallow period i. e. following harvest, were negative for all treatments; the CH_4 uptake was equivalent to between 1 % and 3 % of the annual emissions. Across the whole experiment, the RM+min treatment had lowest annual average CH_4 fluxes (Fig. 4, treatment means: RM+min: $2.44 \text{ g CH}_4\cdot\text{m}^{-2}\cdot\text{a}^{-1}$; RH: $6.20 \text{ g CH}_4\cdot\text{m}^{-2}\cdot\text{a}^{-1}$; RM: $6.36 \text{ g CH}_4\cdot\text{m}^{-2}\cdot\text{a}^{-1}$) though treatment means were not significantly different from one another ($\chi^2(2) = 4.19$, $P = 0.123$).

A non-linear relationship between CH_4 fluxes and chamber temperature (Fig. S11) was identified. Below $12.5 \text{ }^\circ\text{C}$, the maximum hourly flux was $0.013 \text{ mg CH}_4\cdot\text{m}^{-2}$ and above $12.5 \text{ }^\circ\text{C}$ fluxes reached $97.1 \text{ mg CH}_4\cdot\text{m}^{-2}\cdot\text{h}^{-1}$. No significant relationship between CH_4 fluxes and temperature was identified (linear model: $\log_{10}(\text{fluxes} + 0.06) \sim \text{temperature}$; $P > 0.05$).

In the grass plots, CH_4 fluxes (Fig. S6) were close to zero (5th and 95th percentiles of all measurements: -0.041 and $0.013 \text{ mg CH}_4\cdot\text{m}^{-2}\cdot\text{h}^{-1}$, respectively) and the mean seasonal flux was negative at $-0.040 \text{ g CH}_4\cdot\text{m}^{-2}\cdot\text{season}^{-1}$ (range of plot means: -0.057 to $-0.030 \text{ g CH}_4\cdot\text{m}^{-2}\cdot\text{season}^{-1}$).

3.2. N_2O fluxes

N_2O fluxes in rice were highest following fertilisation events (all treatments) and, for the RM treatment, following rainfall events (8th June, 30th August) and the pre-harvest drainage (27th September) (Fig. 5). In total, the N_2O -N losses represent 0.51–1.8 % of the N added to the plots through fertiliser. No emission peaks following the mid-season drainage of the RH plots (4th to 12th August) were identified. The last high fluxes were measured 15 days after the beginning of the pre-harvest drainage (in the RM treatment). From 11th October onwards, fluxes across all rice treatments remained below $0.04 \text{ mg N}_2\text{O}\cdot\text{m}^{-2}\cdot\text{h}^{-1}$ (Fig. 5). Fluxes during the fallow period contributed to 7 % (RH), 16 % (RM) and 44 % (RM+min) of the annual emissions.

The mean annual flux of the RM+min treatment ($56 \text{ mg N}_2\text{O}\cdot\text{m}^{-2}\cdot\text{a}^{-1}$) was significantly lower than that of the RH treatment ($203 \text{ mg N}_2\text{O}\cdot\text{m}^{-2}\cdot\text{a}^{-1}$; $P = 0.037$, Table 1) and lower, though not significantly, than

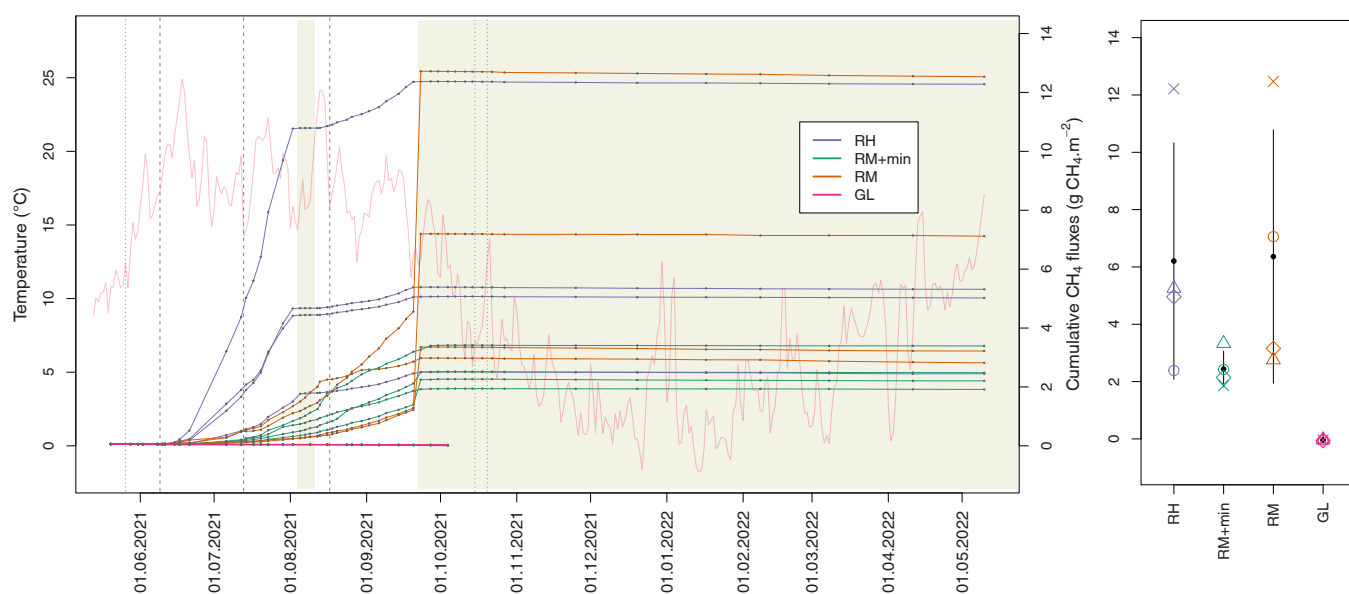


Fig. 4. CH_4 fluxes ($\text{g CH}_4\cdot\text{m}^{-2}$), showing cumulative fluxes through time (left-hand graph) and annual fluxes of the rice and seasonal fluxes of grass plots (treatment means = black dots; vertical lines = 95 % confidence intervals) (right-hand graph); RH = rice plots with a high water table (WT); RM+min = rice plots with a medium WT with mineral cover; RM = rice plots with a medium WT; GL = grass plots with a low WT; the different lines (left-hand graph) and symbols (right-hand graph) show the different plots (4 per treatment); mean daily temperature shown in pink; fertilisation events shown as vertical dashed lines, planting out of rice plants indicated as a vertical dotted line (end of May), harvest dates shown as vertical dotted lines (mid-October); the beige background shows periods during which either the RH plots were drained (mid-season drainage, early August) or all plots were drained (late September onwards).

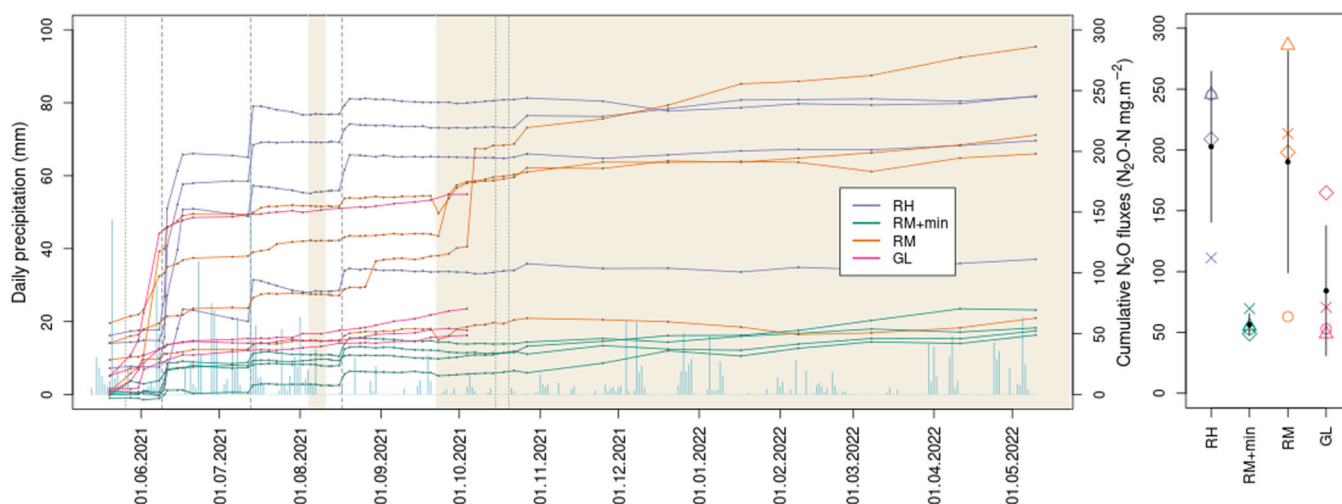


Fig. 5. N_2O fluxes ($\text{mg N}_2\text{O-N.m}^{-2}$) showing cumulative fluxes through time (left-hand graph) and annual fluxes of the rice and seasonal fluxes of grass plots (treatment means = black dots; vertical lines = 95 % confidence intervals) (right-hand graph); RH = rice plots with a high water table (WT); RM+min = rice plots with a medium WT with mineral cover; RM = rice plots with a medium WT; GL = grass plots with a low WT; the different lines (left-hand graph) and symbols (right-hand graph) show the different plots (4 per treatment); daily precipitation shown in turquoise; fertilisation events shown as vertical dashed lines, planting out of rice plants indicated as a vertical dotted line (end of May), harvest dates shown as vertical dotted lines (mid-October); the beige background shows periods during which either the RH plots were drained (mid-season drainage, early August) or all plots were drained (late September onwards).

Table 1

Mean (and 95 % CI) annual CH_4 and N_2O emissions from the rice treatments, as well as their increase in emissions compared to those of the grass treatment ("Additional emissions"), in CO_2 -equivalent; and mean (and standard deviation, $n = 4$) of proportion (and standard deviation, $n = 4$) of annual N_2O emissions identified as fertilisation induced; RH = rice plots with a high water table (WT); RM+min = rice plots with a medium WT with mineral cover; RM = rice plots with a medium WT; GL = grass plots with a low WT; letters in superscript indicate significant differences between mean annual emissions of rice treatments, as described in main text.

	Annual CH_4 emissions ($\text{t CO}_2\text{-eq.ha}^{-1}\text{.a}^{-1}$)	Annual N_2O emissions ($\text{t CO}_2\text{-eq.ha}^{-1}\text{.a}^{-1}$)	Combined CH_4 and N_2O emissions	Additional CH_4 and N_2O emissions*	Fertilisation peaks (%)
RH	1.74 (0.58, 2.89) ^a	0.87 (0.60, 1.14) ^a	2.61 (1.19, 4.03)	2.26 (1.07, 3.45)	87.3 (15.3)
RM+min	0.68 (0.51, 0.86) ^a	0.24 (0.20, 0.28) ^b	0.92 (0.71, 1.14)	0.57 (0.56, 0.59)	59.7 (22.4)
RM	1.78 (0.54, 3.02) ^a	0.82 (0.42, 1.21) ^{ab}	2.60 (0.97, 4.23)	2.25 (0.85, 3.64)	11.0 (10.0)
GL	- 0.01 (- 0.014, - 0.0078)	0.36 (0.13, 0.59)	0.35 (0.12, 0.58)	-	None identified

* = the sum of CH_4 and N_2O emissions ($\text{CO}_2\text{-eq.}$) from each treatment minus the sum of CH_4 and N_2O ($\text{CO}_2\text{-eq.}$) emissions from the GL treatment.

that of the RM treatment ($190 \text{ mg N}_2\text{O-N.m}^{-2}\text{.a}^{-1}$; $P = 0.124$; Table 1, Fig. 5). The contribution of fertiliser-induced peaks to the annual N_2O emissions was variable (Table 1). The RM treatment had high fluxes following the pre-harvest drainage that were not associated with fertilisation (Fig. 5).

The mean seasonal N_2O flux from the grass plots was 84 (range: 53–165) $\text{mg N}_2\text{O-N.m}^{-2} \text{ season}^{-1}$. With one exception, all flux measurements were below $0.24 \text{ mg N}_2\text{O-N.m}^{-2}\text{.ha}^{-1}\text{.h}^{-1}$ (Fig. S10). No fertiliser-induced N_2O peaks were identified.

4. Discussion

4.1. CH_4 emissions

Reported annual or seasonal CH_4 emissions from flooded rice cultivation in the literature are very variable, in part because there are several important drivers of fluxes, including water management, organic amendments, soil type, previous land use, organic matter content and climate. Ranges of CH_4 emissions from other regions in the same climate zone include $17\text{--}367 \text{ kg CH}_4\text{.ha}^{-1}\text{.a}^{-1}$ for N Japan (5th and 95th percentiles for sites without straw addition, Kajiura et al., 2018) and $14\text{--}208 \text{ kg CH}_4\text{.ha}^{-1}\text{.season}^{-1}$ for NE China (range of values, sites without straw addition, Wang et al., 2018). Our annual fluxes ($24\text{--}64 \text{ kg CH}_4\text{.ha}^{-1}\text{.a}^{-1}$, Fig. 4) fall within the range of these values but are at the lower end. This might be explained by several reasons. First, our site has cooler summers than those of the above-cited regions (mean June, July, August temperatures of our site: $17.5, 19.2, 18.7 \text{ }^\circ\text{C}$ [1991–2020], $19.0, 18.3, 17.4 \text{ }^\circ\text{C}$ [2021, MeteoSwiss]; Hokkaido, Japan: $17.0, 21.1, 22.3 \text{ }^\circ\text{C}$ [1991–2020, Japan Meteorological Agency]; Jilin, NE China: $19.5, 22.3, 21.1 \text{ }^\circ\text{C}$ [1991–2021, climate-data.org]) which can be expected to lower CH_4 emissions (Yvon-Durocher et al., 2014). Differences in climate can also explain the lower annual CH_4 emissions measured in this study compared to that calculated using the IPCC Tier 1 approach for Europe (161 [95 % CI: $82\text{--}315$] $\text{kg CH}_4\text{.ha}^{-1}\text{.a}^{-1}$, Hergoualc'h et al., 2019); the sites used to calibrate this IPCC function are situated exclusively in the Mediterranean region (Wang et al., 2018), with hot summers. This highlights the need for measurements in a wider range of climate regions so that emissions from rice cultivation in Europe outside of the Mediterranean region can be estimated adequately. Second, the water level even in the RH rice treatment was high but not flooded, meaning there was a zone in the soil where methanotrophy could have occurred, thus lowering emissions in our experiment. Third, the experiment was carried out during the first occurrence of water-logged conditions on this soil (in the mesocosm experiment). This is relevant because lower CH_4 emissions in the first year of measurements (following dry cultivation) have been observed in other studies (e.g. Hatala et al., 2012; Lagomarsino et al., 2016). Hatala et al. (2012) explained low CH_4 emissions in the first year of measurements by the lack of labile C substrate in the soil. This explanation might apply to our study as although plots were cultivated (grass) in 2020, this organic matter might have been

decomposed aerobically in the fallow months prior to flooding. Lago-marsino et al. (2016) explained their observation of low CH₄ emissions in the first year by the delayed adaptation of the microbial community to anaerobic conditions. This explanation is compatible with our experiment and implies that measurements from this site in future years are necessary to test for the long-term GHG emission effects of wet rice / dry-cultivation rotation and rice monocultures at our study site.

From the beginning of July until mid-season drainage, the RH treatment had the highest CH₄ emissions (Fig. 3). This is most likely explained by the higher WT of this treatment (Fig. 1) but the higher biomass of plants from this treatment (Table S2) might have also contributed to these higher emissions. Mid-season drainage worked well to reduce CH₄ emissions from the RH treatment, both during the drainage period and for several weeks afterwards (Fig. 3). The reduction in VWC for two of the four plots was < 18 % (Fig. 1), lower than that reported in another study (40–60 %, Linquist et al., 2015). This demonstrates that even in organic soils that retain high VWC following drainage, CH₄ emission reductions can be reached with temporary drainage.

The lowest annual CH₄ flux was recorded from the RM+min treatment. One interpretation might be that the mineral cover reduced CH₄ emissions in these water-logged conditions due to lower C content in the upper soil layer of this treatment. However, with the exception of measurements from a single day (following pre-harvest drainage, see below), fluxes from the RM treatment were similarly low (Fig. 3). It is therefore difficult to explain the cause of the lower annual CH₄ emissions in the RM+min treatment.

The high CH₄ peaks following pre-harvest drainage (end of September) recorded from two plots in the RM treatment caused the mean annual emission estimate of this treatment to be as high as that of the RH treatment (Fig. 4). This suggests that eliminating these temporary fluxes is important. High emissions from rice fields following drainage have been recorded also in other studies (e.g. Wassmann et al., 2000; Hatala et al., 2012; Linquist et al., 2015). These large emission peaks are explained as the release of trapped methane due to reduced pressure upon drainage, alongside a low rate of methanotrophy due to both the more rapid movement of the CH₄ through the soil profile and the persistent low redox potential of soil initially following drainage (Denier van der Gon et al., 1996; Han et al., 2005). Consequently, slow decrease in the water table, causing a gradual reduction in pressure, might avoid such post-drainage peaks, substantially reducing the annual GHG balance of this system.

We did not identify a relationship between soil temperature and CH₄ emissions during the growing season, as might be expected based on the close relationship between temperature and annual fluxes (Yvon-Durocher et al., 2014). It suggests that within our system, temperature is not a major driving factor of seasonal CH₄ emission dynamics.

4.2. N₂O emissions

Annual N₂O emissions from the rice treatments of 0.56–2.03 kg N₂O-N.ha⁻¹.a⁻¹ fall between emission factors from (drained) grassland and semi-natural / rewetted land use types (Freeman, 2022), as well as within the range of annual emissions from N Japan (mean [range]: 1 [0.1–3.9] kg N₂O-N.ha⁻¹.a⁻¹, Kajiura et al., 2018). The emissions are lower than the IPCC estimate for drained agriculturally-managed organic soils (8.2–13 kg N₂O-N.ha⁻¹.a⁻¹, Drösler et al., 2014) but this can be explained by the lower C (and thus N) availability in the soils in our study, where much organic matter was protected by anoxic conditions due to water logging, reducing microbial organic matter decomposition rates.

Annual N₂O emissions recorded from the rice plots were lower for the RM+min treatment than the RH and RM treatments (72 % and 70 % lower, respectively). These results support the findings of a field experiment in eastern Switzerland (Wang et al., 2022) which found a 84–90 % reduction of N₂O emissions after mineral coverage on an

intensively managed meadow on organic soil over two years. Though the reduction measured in our study is somewhat lower, it is still a substantial reduction, and shows that the effect holds for organic soil with a near-surface water level. Wang et al. (2022) suggested several explanations for the lower emissions in covered soils, including lower soil organic C content and higher pH in the upper soil layer. These two explanations are supported by our results. The lower soil organic carbon content is especially relevant in this experiment because the peat in the RM+min treatment was completely submerged in water, meaning the main C source was the C-poor mineral cover layer. Additionally, the different water levels might also offer an explanation. Higher N₂O emissions following N inputs are expected for soils near the saturated water-filled pore space (WFPS) (Bateman and Baggs, 2005). Indeed, the VWC of the RM+min treatment (at 5 cm below soil surface) was consistently lower than that of the two other rice treatments. However, because we do not have information on the porosity of the soils, it is not possible to estimate WFPS. This would be important in follow-up studies, because the (expected) lower porosity of the mineral soil might compensate for its lower VWC, resulting in a similar WFPS. In short, the lower N₂O emissions from the RM+min treatment might be the higher pH, the lower C availability, or possibly the lower WFPS. Based on our experimental design however, we cannot disentangle these mechanisms.

Fertiliser peaks accounted for more than half of annual emissions from the RH and RM+min plots (Table 1, Fig. 5), suggesting an important role of N inputs in these treatments. Fertiliser peaks also occurred in the RM treatment (Fig. 5), though they did not account for such a high proportion of annual emissions (11 %). This low value was mostly due to high N₂O fluxes not associated with fertilisation. These occurred a) after the automated water control had been switched on then off then on in mid-May, and b) following the pre-harvest drainage (Fig. 5). Varying water levels have been shown to increase N₂O emissions in several studies (e.g. Beare et al., 2009; Harrison-Kirk et al., 2013). This possible explanation however applies to all rice treatments, and leaves the question unanswered as to why these non-fertiliser peaks were so prominent in the RM treatment. Understanding these emission peaks is important, as they made up a large proportion of the annual N₂O fluxes of this treatment (Fig. 5). Unlike in other studies (e.g. Lago-marsino et al., 2016) the mid-season drainage did not cause enhanced N₂O emissions. In our study site there is thus no indication that this measure, used to reduce CH₄ emissions, increases N₂O emissions.

The GL plots did not show any fertiliser peaks. This might be due to fact that they received in the field only about a quarter as much N as the rice treatments did (GL: 26 kg N.ha⁻¹, rice: 110 kg N.ha⁻¹). Correspondingly, the annual N₂O emission of the GL treatment was less than half of that of the two rice treatments with the same soil (RH and RM), though the variability between plots was large (Fig. 5).

4.3. Climate-friendlier organic soil cultivation

The additional CH₄ and N₂O emissions from the rice treatments, compared to grass control plots were generally low (Table 1). The CH₄ and N₂O emissions from the GL treatment fall within the range of annual emissions from a recent study of drained organic soils in Germany (Tiemeier et al., 2020), considering fluxes from only those (33) grassland sites receiving < 100 kg annual N inputs: 5th and 95th percentile CH₄ emissions: – 5.0–67.3 kg CH₄.ha⁻¹.a⁻¹; 5th and 95th percentile of N₂O-N losses: 0.28–10.4 kg N₂O-N.ha⁻¹.a⁻¹). Although our annual flux estimates are at the lower ends of these ranges, this – and similar results from the rice treatments – implies that our mesocosm experiment is suitable for comparing GHG emissions between different treatments.

In order to compare the overall GHG balance of these treatments however, information on CO₂ emissions is necessary. Although we did not measure net CO₂ emissions, a statistical relationship between water table depth (WTD) and net CO₂ emissions allows the potential CO₂ savings associated with a change from deeply drained grassland to wet

rice production to be estimated. For example [Tiemeyer et al. \(2020\)](#) use a sigmoidal function to describe the net CO₂ emissions based on WTD, based on data from 188 sites in Germany (mixed land use), given in [Eq. 1](#).

$$CO_2 - C(WT) = CO_2 - C_{min} + CO_2 - C_{diff} \times e^{-ae^{bWT}} \quad (1)$$

where $CO_2 - C(WT)$ is the annual CO₂ - C loss (t C.ha⁻¹.a⁻¹) for a given WTD (m), $CO_2 - C_{min}$ is the lower asymptote of CO₂ - C loss (− 0.93 t C.ha⁻¹.a⁻¹), $CO_2 - C_{diff}$ is the difference between the lower and upper (11.00 t C.ha⁻¹.a⁻¹) asymptotes, $a = 7.52$ and $b = 12.97 \text{ m}^{-1}$ ([Tiemeyer et al., 2020](#)). The function estimated emissions of ca. 37 t CO₂.ha⁻¹.a⁻¹ for deeply drained soils, ca. − 3.4 t CO₂.ha⁻¹.a⁻¹ for flooded soils, and a steep decline in emissions between water levels of ca. − 30 cm and − 10 cm ([Tiemeyer et al., 2020](#)). The WTDs recorded from our experiment can thus be used to predict the CO₂ emissions from our four treatments. Two adjustments however need to be made. First, assuming the volume of aerated peat is relevant for the function relating WTD to CO₂ emissions, we set the WTD of the RM+min treatment to be 0 cm, because the peat in this treatment was entirely submerged in water. Second, the wettest sites in [Tiemeyer et al. \(2020\)](#) data set, for which the function predicts negative CO₂ emissions, were near-natural. Such sites might have negative net CO₂ emissions in part because vegetation of near-natural peatlands tends to produce dead organic matter relatively resilient to decomposition. This is not the case for our plots therefore we set the CO₂ emissions of the RM+min and RH treatments to be zero, rather than negative.

Using the [Tiemeyer et al. \(2020\)](#) function to predict the CO₂ emissions from the four treatments from this study results in much higher CO₂ emissions from the GL treatment, than the rice treatments ([Table 2](#)). Combining estimated CO₂ emissions with the CH₄ and N₂O from our measurements allows the CO₂-eq. savings obtained by cultivating wet rice instead of (dry) grass to be calculated. This is done by deducting the CH₄, N₂O ([Table 1](#)) and CO₂ emissions of the GL control treatment from those of the rice treatments. Total emissions from the GL treatment are estimated to be 37.3 t CO₂-eq.ha⁻¹.a⁻¹ and the rice treatments are estimated to have 93 % (RH), 98 % (RM+min) and 60 % (RM) lower GHG emissions. The IPCC CO₂ emission factor for deeply drained nutrient-rich grasslands in the temperate zone is 6.1 t CO₂-eq.ha⁻¹.a⁻¹ ([Drösler et al., 2014](#)), considerably lower than that predicted by [Tiemeyer et al. \(2020\)](#). This discrepancy can be accounted for by calculating the reduction in CO₂ emissions due to the different WTDs of our rice treatments (compared to GL), as described above, and then applying this reduction to the IPCC emission factor (=22.4 t CO₂.ha⁻¹.a⁻¹) instead of the CO₂ emission factor from [Tiemeyer et al. \(2020\)](#). Rice treatments are then estimated to have 89 % (RH), 96 % (RM+min) and 56 % (RM) lower GHG emissions than the GL treatment ([Table 2](#)).

In summary, the high savings of the RH and RM+min treatments stem from their high effective water tables, reducing the estimated CO₂ emissions, but without excessively increased CH₄ emissions ([Table 1](#)). Furthermore, our results suggest that the mineral coverage also lowers N₂O and possibly CH₄ emissions, though its effect is secondary to water level increase. The effectiveness of this mitigation measure needs to be tested still in flooded rice. Nonetheless, the observed high GHG savings suggest that even an 8-fold increase (using the IPCC CO₂ emission factor) in CH₄ emissions would still result in emissions savings from the two rice treatments with the highest effective water tables. This value increases to 14-fold if the higher CO₂ emission factor from [Tiemeyer et al. \(2020\)](#) is used.

5. Conclusion

CH₄ and N₂O emissions were measured from wet rice and deeply drained grass grown on organic soil in an outdoor mesocosm experiment in the cool temperate moist zone. For rice, the combined emissions were less than 2.7 t CO₂-eq.ha⁻¹.a⁻¹. The generally low CH₄ and N₂O emissions

Table 2

CO₂ emissions from the four treatments as estimated using [Eq. \(1\)](#) (from [Tiemeyer et al., 2020](#)) in conjunction with estimates of CO₂ emissions from deeply drained grassland from [Tiemeyer et al. \(2020\)](#) or IPCC ([Drösler et al., 2014](#)), see [Section 4.3](#) for details; RH = rice plots with a high water table (WT); RM+min = rice plots with a medium WT with mineral cover; RM = rice plots with a medium WT; GL = grass plots with a low WT.

	CO ₂ emission using Tiemeyer estimate (t CO ₂ -eq.ha ⁻¹ .a ⁻¹)	CO ₂ reduction using Tiemeyer estimate	CO ₂ emission using IPCC estimate	CO ₂ reduction using IPCC estimate
RH	0*	36.96	0*	22.39
RM+min	0*	36.96	0*	22.39
RM	12.27	24.68	7.44	14.95
GL	36.96	–	22.39	–

* The negative CO₂ emissions estimated by [Eq. \(1\)](#) were set to zero (see [Section 4.3](#) for details).

indicate that wet rice cultivation on the investigated organic soils in this climate zone has the potential to reduce the warming induced by agricultural use of these soils, as opposed to conventional (deeply drained) grass cultivation. Estimated CO₂ emissions further support this proposition. Lower emissions (for N₂O, significantly lower) were recorded from the rice treatment that had a 30 cm mineral layer, indicating this management option should be pursued as a potential GHG reduction option. In general, the CH₄ emissions from the rice treatments had a 2–3 times higher warming potential than the N₂O emissions, implying that further improvement of the GHG balance of this system should focus on CH₄ emissions. The very different dynamics of CH₄ emissions in the two rice treatments that had similarly high annual CH₄ fluxes suggest that there are multiple ways of doing this. For the future, we suggest two directions of research for GHG emission from wet rice in this climate zone. First, measuring CO₂ emissions alongside CH₄ and N₂O emissions. Second, how to amend the rate of drainage, to prevent the pre-harvest drainage CH₄ emission peak.

Funding

This research did not receive any specific grant from funding agencies in the public, commercial, or not-for-profit sectors.

Declaration of Competing Interest

The authors declare that they have no known competing financial interests or personal relationships that could have appeared to influence the work reported in this paper.

Data Availability

The data are available from the Mendeley Data Repository.

Acknowledgements

Robin Giger and Markus Jocher are thanked for their generous support in the field and Marcio Dos Reis Martins is thanked for helpful discussions.

Dedication

In memory of Thomas Walter, who inspired the initiation of the experiment.

Appendix A. Supporting information

Supplementary data associated with this article can be found in the online version at [doi:10.1016/j.agee.2023.108641](https://doi.org/10.1016/j.agee.2023.108641).

References

- Bateman, E.J., Baggs, E.M., 2005. Contributions of nitrification and denitrification to N_2O emissions from soils at different water-filled pore space. *Biol. Fert. Soils* 41, 379–388. <https://doi.org/10.1007/s00374-005-0858-3>.
- Beare, M.H., Gregorich, E.G., St-Georges, P., 2009. Compaction effects on CO_2 and N_2O production during drying and rewetting of soil. *Soil Biol. Biochem.* 41, 611–621. <https://doi.org/10.1016/j.soilbio.2008.12.024>.
- Bickel, K., Richards, G., Köhl, M., Rodrigues, R.L.V., 2006. 2006 IPCC Guidelines for National Greenhouse Gas Inventories, Volume 4. IGES, Japan, pp. 1–42.
- Carlson, K.M., Gerber, J.S., Mueller, N.D., Herrero, M., MacDonald, G.K., Brauman, K.A., Havlik, P., O'Connell, C.S., Johnson, J.A., Saatchi, S., West, P.C., 2017. Greenhouse gas emissions intensity of global croplands. *Nat. Clim. Change* 7, 63–68. <https://doi.org/10.1038/nclimate3158>.
- Denier van der Gon, H.A.C., van Breemen, N., Neue, H.-U., Lantin, R.S., Aduna, J.B., Alberto, M.C.R., Wassmann, R., 1996. Release of entrapped methane from wetland rice fields upon soil drying. *Glob. Biogeochem. Cycles* 10, 1–7. <https://doi.org/10.1029/95GB03460>.
- Drösler, M., Verchot, L.V., Freibauer, A., Pan, G., 2014. 2013 Wetlands Supplement to the 2006 IPCC Guidelines for National Greenhouse Gas Inventories. Chapter 2. IPCC, Switzerland, pp. 1–79.
- Evans, C.D., Peacock, M., Baird, A.J., Artz, R.R.E., Burden, A., Callaghan, N., Chapman, P.J., Cooper, H.M., Coyle, M., Craig, E., Cumming, A., Dixon, S., Gauci, V., Grayson, R.P., Helfter, C., Heppell, C.M., Holden, J., Jones, D.L., Kaduk, J., Levy, P., Mathews, R., McNamara, N.P., Misselbrook, T., Oakley, S., Page, S.E., Rayment, M., Ridley, L.M., Stanley, K.M., Williamson, J.L., Worrall, F., Morrison, R., 2021. Overriding water table control on managed peatland greenhouse gas emissions. *Nature* 593, 548–552. <https://doi.org/10.1038/s41586-021-03523-1>.
- Freeman, B.W.J., Evans, C.D., Musarika, S., Morrison, R., Newman, T.R., Page, S.E., Wiggs, G.F.S., Bell, N.G.A., Styles, D., Wen, Y., Chadwick, D.R., Jones, D.L., 2022. Responsible agriculture must adapt to the wetland character of mid-latitude peatlands. *Glob. Chang. Biol.* 28, 3795–3811. <https://doi.org/10.1111/gcb.16152>.
- Frolking, S., Talbot, J., Jones, M.C., Treat, C.C., Kauffman, J.B., Tuittila, E.-S., Roulet, N., 2011. Peatlands in the Earth's 21st century climate system. *Environ. Res.* 19, 371–396. <https://doi.org/10.1139/a11-014>.
- Fuss, R., 2020. gasfluxes: Greenhouse Gas Flux Calculation from Chamber Measurements. R package version 0.4–4.
- Han, G., Yoshikoshi, H., Nagai, H., Yamada, T., Saito, M., Miyata, A., Harazono, Y., 2005. Concentration and carbon isotope profiles of CH_4 in paddy rice canopy: Isotopic evidence for changes in CH_4 emission pathways upon drainage. *Chem. Geol.* 218, 25–40. <https://doi.org/10.1016/j.chemgeo.2005.01.024>.
- Harrison-Kirk, T., Beare, M.H., Meenken, E.D., Condron, L.M., 2013. Soil organic matter and texture affect responses to dry/wet cycles: Effects on carbon dioxide and nitrous oxide emissions. *Soil Biol. Biochem.* 57, 43–55. <https://doi.org/10.1016/j.soilbio.2012.10.008>.
- Hatala, J.A., Detto, M., Sonnentag, O., Deverel, S.J., Verfaillie, J., Baldocchi, D.D., 2012. Greenhouse gas (CO_2 , CH_4 , H_2O) fluxes from drained and flooded agricultural peatlands in the Sacramento-San Joaquin Delta. *Agr. Ecosyst. Environ.* 150, 1–18. <https://doi.org/10.1016/j.agee.2012.01.009>.
- Hergoualc'h, K., Akiyama, H., Bernoux, M., Chirinda, N., del Prado, A., Kasimir, A., MacDonald, J.D., Ogle, S.M., Regina, K., van der Weerden, T.J., 2019. 2019 Refinement to the 2006 IPCC Guidelines for National Greenhouse Gas Inventories, Volume 4. IPCC, Japan, pp. 1–48.
- Humpenöder, F., Karstens, K., Lotze-Campen, H., Leifeld, J., Menichetti, L., Barthelmes, A., Popp, A., 2020. Peatland protection and restoration are key for climate change mitigation. *Environ. Res. Lett.* 15, 104093 <https://doi.org/10.1088/1748-9326/abae2a>.
- Hüppi, R., Felber, R., Krauss, M., Six, J., Leifeld, J., Fuß, R., 2018. Restricting the nonlinearity parameter in soil greenhouse gas flux calculation for more reliable flux estimates. *PLoS One* 13, e0200876. <https://doi.org/10.1371/journal.pone.0200876>.
- Jacot, K., Churko, G., Burri, M., Walter, T., 2018. Reisanbau im Mittelland auf temporär gefluteter Fläche möglich. *Agroscope Transf.* 238, 1–8.
- Kajiura, M., Minamikawa, K., Tokida, T., Shirato, Y., Wagai, R., 2018. Methane and nitrous oxide emissions from paddy fields in Japan: an assessment of controlling factor using an intensive regional data set. *Agr. Ecosyst. Environ.* 252, 51–60. <https://doi.org/10.1016/j.agee.2017.09.035>.
- Knox, S.H., Sturtevant, C., Matthes, J.H., Koteen, L., Verfaillie, J., Baldocchi, D., 2015. Agricultural peatland restoration: effects of land-use change on greenhouse gas (CO_2 and CH_4) fluxes in the Sacramento-San Joaquin Delta. *Glob. Chang. Biol.* 21, 750–765 <https://doi.org/10.1111/gcb.12745>.
- Lagomarsino, A., Agnelli, A.E., Linquist, B., Adviento-Borbe, M.A., Agnelli, A., Gavina, G., Ravaglia, S., Ferrara, R.M., 2016. Alternate wetting and drying of rice reduced CH_4 emissions but triggered N_2O peaks in a clayey soil of central Italy. *Pedosphere* 26, 533–548. [https://doi.org/10.1016/S1002-0160\(15\)60063-7](https://doi.org/10.1016/S1002-0160(15)60063-7).
- Leiber-Sauheitl, K., Fuß, R., Voigt, C., Freibauer, A., 2014. High CO_2 fluxes from grassland on histic Gleysol along soil carbon and drainage gradients. *Biogeosciences* 11, 749–761. <https://doi.org/10.5194/bg-11-749-2014>.
- Leifeld, J., Wüst-Galley, C., Page, S., 2019. Intact and managed peatland soils as a source and sink of GHGs from 1850 to 2100. *Nat. Clim. Change* 9, 945–947. <https://doi.org/10.1038/s41558-019-0615-5>.
- Linquist, B., van Groenigen, K.J., Adviento-Borbe, M.A., Pittelkow, C., van Kessel, C., 2012. An agronomic assessment of greenhouse gas emissions from major cereal crops. *Glob. Chang. Biol.* 18, 194–209. <https://doi.org/10.1111/j.1365-2486.2011.02502.x>.
- Linquist, B.A., Anders, M.M., Adviento-Borbe, M.A., Chaney, R.L., Nalley, L.L., da Rosa, E.F., van Kessel, C., 2015. Reducing greenhouse gas emissions, water use, and grain arsenic levels in rice systems. *Glob. Chang. Biol.* 21, 407–417. <https://doi.org/10.1111/gcb.12701>.
- Maclean, J.L., Dawe, D.C., Hardy, B., Hettel, G.P. (Eds.), 2002. *Rice Almanac*. CABI, Oxfordshire, UK vii + 253.
- Maier, M., Weber, T.K.D., Fiedler, J., Fuß, R., Glatzel, S., Huth, V., Jordan, S., Jurasinski, G., Kutzbach, L., Schäfer, K., Weymann, D., Hagemann, U., 2022. Introduction of a guideline for measurements of greenhouse gas fluxes from soils using non-steady-state chambers. *J. Plant Nutr. Soil Sc.* 185, 447–461. <https://doi.org/10.1002/jpln.202200199>.
- Ocko, I.B., Sun, T., Shindell, D., Oppenheimer, M., Hristov, A.N., Pacala, S.W., Mauzerall, D.L., Xu, Y., Hamburg, S.P., 2021. Acting rapidly to deploy readily available methane mitigation measures by sector can immediately slow global warming. *Environ. Res. Lett.* 16, 054042 <https://doi.org/10.1088/1748-9326/abf9c8>.
- Paul, S.M., Leifeld, J., 2022. In: Rumpel, C. (Ed.), *Management of Organic Soils to Reduce Soil Organic Carbon Losses. Understanding and fostering soil carbon sequestration* Burleigh Dodds Science Publishing Limited, Cambridge, UK, pp. 617–680.
- Richner, W., Sinaj, S., 2017. *Grundlagen für die Düngung landwirtschaftlicher Kulturen in der Schweiz*. Agrar. Schweiz 8, 1–276.
- Saunio, M., Stavert, A.R., Poulter, B., Bousquet, P., Canadell, J.G., Jackson, R.B., Raymond, P.A., Dlugokencky, E.J., Houweling, S., Patra, P.K., Ciais, P., Arora, V.K., Bastviken, D., Bergamaschi, P., Blake, D.R., Brailsford, G., Bruhwiler, L., Carlson, K.M., Carrol, M., Castaldi, S., Chandra, N., Crevoisier, C., Crill, P.M., Covey, K., Curry, C.L., Etiope, G., Frankenberg, C., Gedney, N., Hegglin, M.L., Höglund-Isaksson, L., Hugelius, G., Ishizawa, M., Ito, A., Janssens-Maenhout, G., Jensen, K.M., Joos, F., Kleinen, T., Krummel, P.B., Langenfelds, R.L., Laruelle, G.G., Liu, L., Machida, T., Maksyutov, S., McDonald, K.C., McNorton, J., Miller, P.A., Melton, J.R., Morino, I., Müller, J., Murguía-Flores, F., Naik, V., Niwa, Y., Noce, S., O'Doherty, S., Parker, R.J., Peng, C., Peng, S., Peters, G.P., Prigent, C., Prinn, R., Ramonet, M., Regnier, P., Riley, W.J., Rosentretter, J.A., Segers, A., Simpson, I.J., Shi, H., Smith, S.J., Steele, L.P., Thornton, B.F., Tian, H., Tohjima, Y., Tubiello, F.N., Tsuruta, A., Viovy, N., Voulgarakis, A., Weber, T.S., van Weele, M., van der Werf, G.R., Weiss, R. F., Worthy, D., Wunch, D., Yin, Y., Yoshida, Y., Zhang, W., Zhang, Z., Zhao, Y., Zheng, B., Zhu, Q., Zhu, Q., Zhuang, Q., 2020. The Global Methane Budget 2000–2017. *Earth Syst. Sci. Data* 12, 1561–1623. <https://doi.org/10.5194/essd-12-1561-2020>.
- Smith, C., Nicholls, Z.R.J., Armour, K., Collins, W., Forster, P., Meinshausen, M., Palmer, M.D., Watanabe, M., 2021. The earth's energy budget, climate feedbacks, and climate sensitivity supplementary material. In: Masson-Delmotte, V., Zhai, P., Pirani, A., Connors, S.L., Péan, C., Berger, S., Caud, N., Chen, Y., Goldfarb, L., Gomis, M.L., Huang, M., Leitzell, M., Lonnoy, E., Matthews, J.B.R., Maycock, T.K., Waterfield, T., Yelekçi, O., Yu, R., Zhou, B. (Eds.), *Climate Change 2021: The Physical Science Basis. Contribution of Working Group I to the Sixth Assessment Report of the Intergovernmental Panel on Climate Change*. Cambridge University Press, Cambridge, United Kingdom and New York, NY, USA, pp. 1–2391. <https://doi.org/10.1017/9781009157896>.
- Tiemeyer, B., Freibauer, A., Borraz, E.A., Augustin, J., Bechtold, M., Beetz, S., Beyer, C., Ebli, M., Eickenscheidt, T., Fiedler, S., Förster, C., Gensior, A., Giebels, M., Glatzel, S., Heinichen, J., Hoffmann, M., Höper, H., Jurasinski, G., Lagner, A., Leiber-Sauheitl, K., Peichl-Brak, M., Drösler, M., 2020. A new methodology for organic soils in national greenhouse gas inventories: data synthesis, derivation and application. *Ecol. Indic.* 109, 105838 <https://doi.org/10.1016/j.ecolind.2019.105838>.
- Verhoeven, J.T.A., Setter, T.L., 2010. Agricultural use of wetlands: opportunities and limitations. *Ann. Bot.-Lond.* 105, 155–163. <https://doi.org/10.1093/aob/mcp172>.
- Wang, J., Akiyama, H., Yagi, K., Yan, X., 2018. Controlling variables and emission factors of methane from global rice fields. *Atmos. Chem. Phys.* 18, 10419–10431. <https://doi.org/10.5194/acp-18-10419-2018>.
- Wang, Y., Paul, S.M., Jocher, M., Alewell, C., Leifeld, J., 2022. Reduced nitrous oxide emissions from drained temperate agricultural peatland after coverage with mineral soil. *Front. Environ. Sci.* 10. <https://doi.org/10.3389/fenvs.2022.856599>.
- Wassmann, R., Neue, H.U., Lantin, R.S., Makarim, K., Chareonsilp, N., Buendia, L.V., Rennenberg, H., 2000. Characterization of methane emissions from rice fields in Asia. II. Differences among irrigated, rainfed, and deepwater rice. *Nutr. Cycl. Agroecosyst.* 58, 13–22. <https://doi.org/10.1023/A:1009822030832>.
- Wichtmann, W., Schröder, C., Joosten, H. (Eds.), 2016. *Paludiculture - Productive Use of Wet Peatlands*. Schweizerbart Scientific Publishers, Stuttgart, Germany viii + 272.
- Wijedasa, L.S., Page, S.E., Evans, C.D., Osaki, M., 2016. Time for responsible peatland agriculture. *Science* 354. <https://doi.org/10.1126/science.aall794>, 562–562.
- Yvon-Durocher, G., Allen, A.P., Bastviken, D., Conrad, R., Gudasz, C., St-Pierre, A., Thanh-Duc, N., del Giorgio, P.A., 2014. Methane fluxes show consistent temperature dependence across microbial to ecosystem scales. *Nature* 507, 488–491. <https://doi.org/10.1038/nature13164>.
- Zou, J., Ziegler, A.D., Chen, D., McNicol, G., Ciais, P., Jiang, X., Zheng, C., Wu, J., Wu, J., Lin, Z., He, X., Brown, L.E., Holden, J., Zhang, Z., Ramchunder, S.J., Chen, A., Zeng, Z., 2022. Rewetting global wetlands effectively reduces major greenhouse gas emissions. *Nat. Geosci.* 15, 627–632. <https://doi.org/10.1038/s41561-022-00989-0>.